



HAL
open science

Amplitude-modulated acoustic radiation force experienced by elastic and viscoelastic spherical shells in progressive waves

F.G. Mitri, Zine El Abiddine E.A. Fellah

► **To cite this version:**

F.G. Mitri, Zine El Abiddine E.A. Fellah. Amplitude-modulated acoustic radiation force experienced by elastic and viscoelastic spherical shells in progressive waves. *Ultrasonics*, 2006, 44 (3), pp.287-296. 10.1016/j.ultras.2006.03.001 . hal-00105784

HAL Id: hal-00105784

<https://hal.science/hal-00105784>

Submitted on 16 Jun 2022

HAL is a multi-disciplinary open access archive for the deposit and dissemination of scientific research documents, whether they are published or not. The documents may come from teaching and research institutions in France or abroad, or from public or private research centers.

L'archive ouverte pluridisciplinaire **HAL**, est destinée au dépôt et à la diffusion de documents scientifiques de niveau recherche, publiés ou non, émanant des établissements d'enseignement et de recherche français ou étrangers, des laboratoires publics ou privés.



Distributed under a Creative Commons Attribution - NonCommercial 4.0 International License

Amplitude-modulated acoustic radiation force experienced by elastic and viscoelastic spherical shells in progressive waves

F.G. Mitri ^{a,*}, Z.E.A. Fellah ^b

^a Mayo Clinic College of Medicine, Department of Physiology and Biomedical Engineering, Ultrasound Research Laboratory, 200 First Street SW, Rochester MN 55905, USA

^b Laboratoire de Mécanique et d'Acoustique, CNRS-UPR 7051, 31 Chemin Joseph Aiguier, Marseille 13009, France

The dynamic acoustic radiation force resulting from a dual-frequency beam incident on spherical shells immersed in an inviscid fluid is examined theoretically in relation to their thickness and the contents of their interior hollow regions. The theory is modified to include a hysteresis type of absorption inside the shells' material. The results of numerical calculations are presented for stainless steel and absorbing lucite (PolyMethyMethacrylAte) shells with the hollow region filled with water or air. Significant differences occur when the interior fluid inside the hollow region is changed from water to air. It is shown that the dynamic radiation force function Y_d deviates from the static radiation force function Y_p when the modulation size parameter $\delta x = |x_2 - x_1|$ ($x_1 = k_1 a$, $x_2 = k_2 a$, k_1 and k_2 are the wave vectors of the incident ultrasound waves, and a is the outer radius of the shell) starts to exceed the width of the resonance peaks in the Y_p curves.

Keywords: Acoustic scattering; Amplitude-modulated radiation force; Nonlinear acoustics

1. Introduction

The acoustic radiation force is a phenomenon associated with the propagation of acoustic waves from one medium to another [1] as a result of nonlinear (second-order) effects. It is caused by a transfer of momentum from the wave to the medium, arising either from absorption or reflection of the wave in or at the second medium. This momentum transfer results in the application of a force in the direction of wave propagation and in another transverse to it [2]. The magnitude of this force is dependent upon both the medium properties and the acoustic beam parameters. The duration of the force application is determined by the temporal profile of the acoustic wave. Generally speaking, radiation force is a mean *steady* force [3–8] which, under

the conditions at which it is measured, depends on the difference in the energy densities on the two sides of the target. A detailed theoretical study on a rigid sphere was developed [9] and extended [10] to include the effect of the sphere's compressibility. Later, Hasegawa and Yosioka [11] provided theoretical and experimental work on the radiation force experienced by an isotropic elastic sphere in a plane progressive wave. Moreover, theories were developed to study the acoustic radiation force due to progressive [12–14] and standing [15–17] plane waves on elastic and viscoelastic spherical, cylinders, and cylindrical shells as well as on coated spheres [18].

Interesting studies revealing new effects of the amplitude modulated acoustic radiation force (for standing waves) on drops and bubbles were performed [19,20] and found to be useful in acoustic levitation applications.

The stress resulting from the acoustic radiation force in solids was examined theoretically [21] and experimentally

* Corresponding author. Tel.: +1 507 2848810; fax: +1 507 2660561.
E-mail addresses: mitri@ieee.org, mitri.farid@mayo.edu (F.G. Mitri).

[22]. In those studies, it was found that the radiation stress depends on both the acoustic nonlinear parameter, which characterizes the stress nonlinearity in the object, and the energy density of the acoustical wave.

The influence of dissipative effects, such as viscosity and heat-conduction, were also studied and it was found that they drastically influence the acoustic radiation force; its magnitude and sign become different from those predicted by the classical theories neglecting losses [23].

In all the studies mentioned above, the incident field is considered to be continuous with constant amplitude, thus radiation force was defined as a *static* force. One may define the *dynamic* (or amplitude-modulated) radiation force as a continuous wave whose intensity varies slowly with time [24]. In such a case, the radiation force on the object will follow the temporal variations of the incident intensity field. This can be achieved in various ways. For example, one can use a single ultrasound beam whose amplitude is modulated at low frequency, or two interfering ultrasound beams (*dual mode*) driven at slightly different frequencies to produce a dynamic radiation force at their intersection. Using a single amplitude modulated beam seems to be the simplest means to produce the oscillatory force. However, such a beam will exert a radiation force on the transducer itself and on any object that is present along the beam path, hence, producing noise. Therefore, the use of the *dual mode* is advantageous to produce a field modulation at the intersection region in a well-confined space.

Actually, dynamic elasticity imaging techniques based on the dynamic radiation force are the subject of extensive experimental investigations [25–28]. In materials science the dynamic radiation force is used in determining resonance frequencies of differently shaped objects [29], evaluating Young’s modulus [30], and estimating porosity [31]. Moreover, it is studied on solid spheres embedded in a viscoelastic medium; by causing microspheres to vibrate using the dynamic radiation force and measuring their resonance curves (vibrational velocity versus frequency) it was possible to accurately measure the complex shear modulus within gel phantoms [32]. The dynamic radiation force is also applied for medical imaging purposes [33] to control the brachytherapy metal seed implantation treatment for prostate cancer [34].

In spite of the wide experimental use of the dynamic force, only two recent works are done to study the dynamic radiation force on solid cylinders [35], cylindrical shells [36] and spheres [37,38] immersed in ideal fluids. Although the cylinder, sphere and cylindrical shells’ results are useful for many medical applications (see [34] for example), particular interest is concentrated on spherical polymer-shelled contrast agents and micro-bubbles. To the authors’ knowledge, the theory of dynamic radiation force on spherical shells is not developed yet. The development for the theory gives a priori knowledge for the dynamic radiation force magnitude which can be used either non-destructively or destructively on such shell-type objects. In this work, a theoretical study of the dynamic radiation force experienced

by elastic and viscoelastic spherical shells (with hollow) immersed in a nonviscous fluid is developed. The theory is restricted to the radiation force along the direction of wave propagation produced by the *dual ultrasound axisymmetric beams mode* (two axial plane waves intersecting in a small region and producing an amplitude modulated plane wave beam). Since axisymmetric beams are considered here, the transverse averaged-force does not contribute to the total radiation force. In addition, the incident field is assumed to be moderate so that the scattered field from the shells is taken to linear approximation and the scattering of sound by sound (also known as parametric or nonlinear interaction) does not occur. It should be noted here that Rooney [39] has discussed the coupling effect of nonlinearity with the radiation force for moderate waves. His results show that the radiation force is independent of fluid nonlinearity (the magnitude of the variation is within the error of his experiments). In this region, *it is assumed that the wave numbers are coplanar*. Moreover, the shell is considered to be totally placed within the focal zone (Fig. 1). Analytical expressions of the dynamic radiation force experienced by spherical shells are derived. The theory is modified to include the effect of absorption inside the shells’ material. As an example to illustrate the theory, numerical results are performed for stainless steel and absorbent lucite (polymer) spherical shells with emphasis on their thickness and the nonviscous fluid filling their interior hollow spaces.

2. Method

Customarily, radiation force is calculated by integrating the radiation-stress tensor over the surface of the object. A simpler approach is to use Yosioka and Kawasima’s formula [10] which enables the calculation of radiation force from the first-order scattered field over the shell boundary at its equilibrium position. Therefore, the linear scattered field should be calculated first in order to compute the radiation force.

2.1. Acoustic scattering of two plane waves from the spherical shell

The velocity potential of the two plane waves represented in spherical coordinates (r, θ, ϕ) can be written as

$$\phi_i = A \sum_{m=1}^2 \sum_{n=0}^{N \rightarrow \infty} (2n+1)(-i)^n j_n(k_m r) P_n(\cos \theta) e^{i\omega_m t}, \quad (1)$$

where A is the amplitude, k_1 and k_2 are the wave numbers (denoted by k_m , $m = 1, 2$), $j_n(k_m r)$ is the spherical Bessel function of the first kind of order n and argument $k_m r$, and $P_n(\cdot)$ are the Legendre polynomials.

The total wave velocity in the core material of the shell is expressed by [12]

$$\mathbf{v}_{\text{int}} = -\nabla \phi_{\text{int}} + \nabla \times \Psi_{\text{int}}, \quad (2)$$

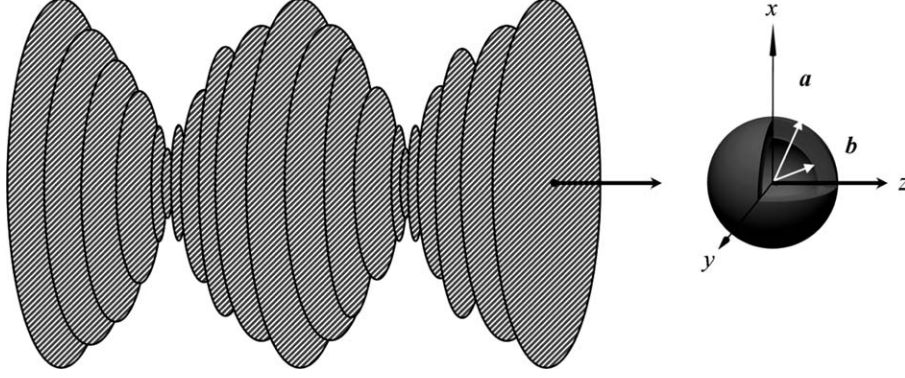


Fig. 1. A spherical shell placed in an amplitude modulated sound beam incident from the direction $\theta = \pi$. The amplitude-modulated field is produced by interfering two confocal sound beams driven at slightly different frequencies.

where ϕ_{int} and $\Psi_{\text{int}}(0, 0, \Psi_{\text{int}})$ are the scalar and vector potentials expressed in spherical coordinates by

$$\begin{aligned} \phi_{\text{int}} &= A \sum_{m=1}^2 \sum_{n=0}^{N \rightarrow \infty} (2n+1)(-i)^n [A_{m,n} j_n(k_{m,l}r) \\ &\quad + B_{m,n} n_n(k_{m,l}r)] P_n(\cos \theta) e^{i\omega_m t}, \\ \Psi_{\text{int}} &= A \sum_{m=1}^2 \sum_{n=0}^{N \rightarrow \infty} (2n+1)(-i)^n [C_{m,n} j_n(k_{m,s}r) \\ &\quad + D_{m,n} n_n(k_{m,s}r)] \frac{d(P_n(\cos \theta))}{d\theta} e^{i\omega_m t}, \end{aligned} \quad (3)$$

where $k_{m,l} = \frac{\omega_m}{c_1}$ is wave number corresponding to the longitudinal wave, c_1 is the longitudinal wave velocity, $k_{m,s} = \frac{\omega_m}{c_s}$ is the wave number corresponding to the shear wave, c_s is the shear wave velocity, $n_n(\cdot)$ is the spherical Bessel function of the second kind, and $A_{m,n}$, $B_{m,n}$, $C_{m,n}$, and $D_{m,n}$ are arbitrary coefficients.

The velocity potential in the fluid filling the hollow space is represented by

$$\phi_3 = A \sum_{m=1}^2 \sum_{n=0}^{N \rightarrow \infty} (2n+1)(-i)^n E_{m,n} j_n(k_{m,3}r) P_n(\cos \theta) e^{i\omega_m t}, \quad (4)$$

where $b_{m,n}$ are unknown coefficients, and $k_{m,3}$ are the wave numbers of each of the waves within the fluid that fills the interior shell's hollow space.

The scattered waves may be expressed as

$$\phi_s = A \sum_{m=1}^2 \sum_{n=0}^{N \rightarrow \infty} (2n+1)(-i)^n S_{m,n} h_n^{(2)}(k_m r) P_n(\cos \theta) e^{i\omega_m t}, \quad (5)$$

where $h_n^{(2)}$ are the spherical Hankel functions of the second kind and $S_{m,n}$ are the scattering coefficients of the first and second wave respectively, to be determined from the boundary conditions (see below) and given by

$$S_{m,n} = \frac{-F_{m,n} j_n(x_m) + x_m j_n'(x_m)}{F_{m,n} h_n^{(2)}(x_m) - x_m h_n^{(2)'}(x_m)}; \quad m = 1, 2, \quad (6)$$

where $x_m = k_m a$, with a being the outer radius of the shell (see Fig. 1). We define the coefficients $\alpha_{m,n}$ and $\beta_{m,n}$ as the real and imaginary parts of $S_{m,n}$, respectively.

The coefficients $F_{m,n}$ are given by

$$F_{m,n} = -\rho \begin{vmatrix} \lambda_{m,22} & \lambda_{m,23} & \lambda_{m,24} & \lambda_{m,25} & 0 \\ \lambda_{m,32} & \lambda_{m,33} & \lambda_{m,34} & \lambda_{m,35} & 0 \\ \lambda_{m,42} & \lambda_{m,43} & \lambda_{m,44} & \lambda_{m,45} & \lambda_{m,46} \\ \lambda_{m,52} & \lambda_{m,53} & \lambda_{m,54} & \lambda_{m,55} & \lambda_{m,56} \\ \lambda_{m,62} & \lambda_{m,63} & \lambda_{m,64} & \lambda_{m,65} & 0 \\ \hline \lambda_{m,12} & \lambda_{m,13} & \lambda_{m,14} & \lambda_{m,15} & 0 \\ \lambda_{m,32} & \lambda_{m,33} & \lambda_{m,34} & \lambda_{m,35} & 0 \\ \lambda_{m,42} & \lambda_{m,43} & \lambda_{m,44} & \lambda_{m,45} & \lambda_{m,46} \\ \lambda_{m,52} & \lambda_{m,53} & \lambda_{m,54} & \lambda_{m,55} & \lambda_{m,56} \\ \lambda_{m,62} & \lambda_{m,63} & \lambda_{m,64} & \lambda_{m,65} & 0 \end{vmatrix}, \quad (7)$$

where ρ is the density of the fluid surrounding the shell.

The coefficients $\lambda_{m,kl}$ defined in Eq. (7) are determined by applying the following boundary conditions [12] at $r = a$ and $r = b$ (Fig. 1); (a and b being the outer and inner radius of the spherical shell, respectively) (1) The pressure in the fluid must be equal to the normal component of stress in the shell at the interface, (2) The normal (radial) component of displacement (or velocity, respectively) of the fluid must be equal to the normal component of displacement (or velocity, respectively) of the shell at the interface, (3) The tangential components of shearing stress must vanish at the surface of the shell. The coefficients $\lambda_{m,kl}$ are explicitly given in reference [12].

The total velocity potential is then:

$$\begin{aligned} \phi &= \phi_i + \phi_s \\ &= A \sum_{m=1}^2 \sum_{n=0}^{N \rightarrow \infty} (2n+1)(-i)^n [U_{m,n}(k_m r) + iV_{m,n}(k_m r)] P_n(\cos \theta) e^{i\omega_m t}, \end{aligned} \quad (8)$$

where $U_{m,n}$, $V_{m,n}$ and their derivatives are defined as

$$\begin{aligned} U_{m,n} &= (1 + \alpha_{m,n})j_n(k_m r) + \beta_{m,n}n_n(k_m r), \\ U'_{m,n} &= \frac{d[U_{m,n}(k_m r)]}{d[k_m r]}, \\ V_{m,n} &= \beta_{m,n}j_n(k_m r) - \alpha_{m,n}n_n(k_m r), \\ V'_{m,n} &= \frac{d[V_{m,n}(k_m r)]}{d[k_m r]}, \end{aligned} \quad (9)$$

where $n_n(\cdot)$ is the spherical Bessel function of the second kind.

From both Eqs. (8) and (9) we have

$$\Psi = \text{Re}[\phi] = A \sum_{n=0}^{N \rightarrow \infty} (2n+1)R_n P_n(\cos \theta), \quad (10)$$

where Re corresponds to the real part of the complex number and R_n is expressed by

$$R_n = \text{Re} \left[\sum_{m=1}^2 (-i)^n [U_{m,n}(k_m r) + iV_{m,n}(k_m r)] e^{i\omega_m t} \right]. \quad (11)$$

2.2. Dynamic radiation force experienced by the spherical shell

The radiation force exerted by a modulated-ultrasound wave is obtained through the short-term time average [27] to discriminate the slow time-variation. The short-term time average of an arbitrary function $\chi(t)$ over the interval of T at time t , is defined as

$$\langle \chi(t) \rangle = \frac{1}{T} \int_{t-T/2}^{t+T/2} \chi(t) dt, \quad (12)$$

where $\frac{2\pi}{\omega_1 + \omega_2} \ll T \ll \frac{2\pi}{|\omega_1 - \omega_2|}$.

Using the formula given by Hasegawa et al. [12] we have

$$\langle F_z \rangle = \langle F_r \rangle + \langle F_\theta \rangle + \langle F_{r,\theta} \rangle + \langle F_t \rangle, \quad (13)$$

where the subscript z refers to the direction of wave propagation (Fig. 1). Inserting Eq. (10) into Eq. (13) we obtain the following components of the force $\langle F_z \rangle$:

$$\begin{aligned} \langle F_r \rangle &= -\pi a^2 \rho \left\langle \int_0^\pi \left(\frac{\partial \Psi}{\partial r} \right)_{r=a}^2 \sin \theta \cos \theta d\theta \right\rangle \\ &= -4\pi a^2 \rho |A|^2 \sum_{n=0}^{N \rightarrow \infty} (n+1) \langle R'_n R'_{n+1} \rangle_{r=a} \\ &= -2\pi \rho |A|^2 \left[\sum_{n=0}^{N \rightarrow \infty} (n+1) \left(\begin{aligned} &x_1^2 (U'_{1,n} V'_{1,n+1} - V'_{1,n} U'_{1,n+1}) + x_2^2 (U'_{2,n} V'_{2,n+1} - V'_{2,n} U'_{2,n+1}) \\ &+ x_1 x_2 (U'_{1,n} U'_{2,n+1} - U'_{2,n} U'_{1,n+1} + V'_{1,n} V'_{2,n+1} - V'_{2,n} V'_{1,n+1}) \sin(\Delta \omega t) \\ &+ x_1 x_2 (U'_{1,n} V'_{2,n+1} + U'_{2,n} V'_{1,n+1} - V'_{1,n} U'_{2,n+1} - V'_{2,n} U'_{1,n+1}) \cos(\Delta \omega t) \end{aligned} \right) \right], \end{aligned} \quad (14)$$

$$\begin{aligned} \langle F_\theta \rangle &= \pi \rho \left\langle \int_0^\pi \left(\frac{\partial \Psi}{\partial \theta} \right)_{r=a}^2 \sin \theta \cos \theta d\theta \right\rangle \\ &= 4\pi \rho |A|^2 \sum_{n=0}^{N \rightarrow \infty} n(n+1)(n+2) \langle R_n R_{n+1} \rangle \\ &= 2\pi \rho |A|^2 \left[\sum_{n=0}^{N \rightarrow \infty} n(n+1)(n+2) \left(\begin{aligned} &(U_{1,n} V_{1,n+1} + U_{2,n} V_{2,n+1} - V_{1,n} U_{1,n+1} - V_{2,n} U_{2,n+1}) \\ &+ (U_{1,n} U_{2,n+1} - U_{2,n} U_{1,n+1} + V_{1,n} V_{2,n+1} - V_{2,n} V_{1,n+1}) \sin(\Delta \omega t) \\ &+ (U_{1,n} V_{2,n+1} + U_{2,n} V_{1,n+1} - V_{1,n} U_{2,n+1} - V_{2,n} U_{1,n+1}) \cos(\Delta \omega t) \end{aligned} \right) \right], \end{aligned} \quad (15)$$

$$\begin{aligned} \langle F_{r,\theta} \rangle &= 2\pi a \rho \left\langle \int_0^\pi \left(\frac{\partial \Psi}{\partial r} \right)_{r=a} \left(\frac{\partial \Psi}{\partial \theta} \right)_{r=a} \sin^2 \theta d\theta \right\rangle \\ &= 4\pi a \rho |A|^2 \sum_{n=0}^{N \rightarrow \infty} [n(n+1) \langle R_n R'_{n+1} \rangle_{r=a} - (n+1)(n+2) \langle R'_n R_{n+1} \rangle_{r=a}] \\ &= 2\pi \rho |A|^2 \sum_{n=0}^{N \rightarrow \infty} (n+1) \left[\begin{aligned} &n \left\{ \begin{aligned} &(x_1 U_{1,n} V'_{1,n+1} + x_2 U_{2,n} V'_{2,n+1} - x_1 V_{1,n} U'_{1,n+1} - x_2 V_{2,n} U'_{2,n+1}) \\ &+ (x_2 U_{1,n} U'_{2,n+1} - x_1 U_{2,n} U'_{1,n+1} + x_2 V_{1,n} V'_{2,n+1} - x_1 V_{2,n} V'_{1,n+1}) \sin(\Delta \omega t) \\ &+ (x_2 U_{1,n} V'_{2,n+1} + x_1 U_{2,n} V'_{1,n+1} - x_2 V_{1,n} U'_{2,n+1} - x_1 V_{2,n} U'_{1,n+1}) \cos(\Delta \omega t) \end{aligned} \right\} \\ &- (n+2) \left\{ \begin{aligned} &(x_1 U'_{1,n} V_{1,n+1} + x_2 U'_{2,n} V_{2,n+1} - x_1 V'_{1,n} U_{1,n+1} - x_2 V'_{2,n} U_{2,n+1}) \\ &+ (x_1 U'_{1,n} U_{2,n+1} - x_2 U'_{2,n} U_{1,n+1} + x_1 V'_{1,n} V_{2,n+1} - x_2 V'_{2,n} V_{1,n+1}) \sin(\Delta \omega t) \\ &+ (x_1 U'_{1,n} V_{2,n+1} + x_2 U'_{2,n} V_{1,n+1} - x_1 V'_{1,n} U_{2,n+1} - x_2 V'_{2,n} U_{1,n+1}) \cos(\Delta \omega t) \end{aligned} \right\} \end{aligned} \right], \end{aligned} \quad (16)$$

and

$$\begin{aligned} \langle F_t \rangle &= -\frac{\pi a^2 \rho}{c^2} \left\langle \int_0^\pi \left(\frac{\partial \Psi}{\partial t} \right)_{r=a}^2 \sin \theta \cos \theta d\theta \right\rangle = -\frac{4\pi a^2 \rho |A|^2}{c^2} \sum_{n=0}^{N \rightarrow \infty} (n+1) \left\langle \frac{\partial R_n}{\partial t} \frac{\partial R_{n+1}}{\partial t} \right\rangle \\ &= -2\pi \rho |A|^2 \left[\sum_{n=0}^{N \rightarrow \infty} (n+1) \left(\begin{aligned} &x_1^2 (U_{1,n} V_{1,n+1} - V_{1,n} U_{1,n+1}) + x_2^2 (U_{2,n} V_{2,n+1} - V_{2,n} U_{2,n+1}) \\ &+ x_1 x_2 (U_{1,n} U_{2,n+1} - U_{2,n} U_{1,n+1} + V_{1,n} V_{2,n+1} - V_{2,n} V_{1,n+1}) \sin(\Delta \omega t) \\ &+ x_1 x_2 (U_{1,n} V_{2,n+1} + U_{2,n} V_{1,n+1} - V_{1,n} U_{2,n+1} - V_{2,n} U_{1,n+1}) \cos(\Delta \omega t) \end{aligned} \right) \right]. \end{aligned} \quad (17)$$

After replacing Eqs. (14)–(17) in Eq. (13) and manipulating the result, the expression of the radiation force is reduced to

$$\begin{aligned} \langle F_z \rangle &= \pi a^2 \left(\frac{1}{2} \rho k_1^2 |A|^2 \right) Y_{p_1} + \pi a^2 \left(\frac{1}{2} \rho k_2^2 |A|^2 \right) Y_{p_2} \\ &\quad + \pi a^2 (\rho k_1 k_2 |A|^2) \Gamma \sin(\Delta \omega t) \\ &\quad + \pi a^2 (\rho k_1 k_2 |A|^2) A \cos(\Delta \omega t), \end{aligned} \quad (18)$$

where

$$Y_{p_1} = -\frac{4}{x_1^2} \sum_{n=0}^{N \rightarrow \infty} [(n+1)(\alpha_{1,n} + \alpha_{1,n+1} + 2\alpha_{1,n}\alpha_{1,n+1} + 2\beta_{1,n}\beta_{1,n+1})], \quad (19)$$

$$Y_{p_2} = -\frac{4}{x_2^2} \sum_{n=0}^{N \rightarrow \infty} [(n+1)(\alpha_{2,n} + \alpha_{2,n+1} + 2\alpha_{2,n}\alpha_{2,n+1} + 2\beta_{2,n}\beta_{2,n+1})], \quad (20)$$

$$\Gamma = 2 \sum_{n=0}^{N \rightarrow \infty} (n+1) \left\{ \begin{aligned} &[j_n(x_2)j_{n+1}(x_1) - j_n(x_1)j_{n+1}(x_2)](2 + \alpha_{1,n} + \alpha_{1,n+1} + \alpha_{2,n} + \alpha_{2,n+1}) \\ &+ [j_n(x_2)n_{n+1}(x_1) - n_n(x_1)j_{n+1}(x_2)](\beta_{1,n} + \beta_{1,n+1}) \\ &+ [n_n(x_2)j_{n+1}(x_1) - j_n(x_1)n_{n+1}(x_2)](\beta_{2,n} + \beta_{2,n+1}) \\ &+ [j_n(x_2)j_{n+1}(x_1) - j_n(x_1)j_{n+1}(x_2) + n_n(x_2)n_{n+1}(x_1) - n_n(x_1)n_{n+1}(x_2)] \\ &(\alpha_{1,n}\alpha_{2,n+1} + \alpha_{2,n}\alpha_{1,n+1} + \beta_{1,n}\beta_{2,n+1} + \beta_{2,n}\beta_{1,n+1}) \\ &+ [j_n(x_2)n_{n+1}(x_1) - n_n(x_1)j_{n+1}(x_2) + j_n(x_1)n_{n+1}(x_2) - n_n(x_2)j_{n+1}(x_1)] \\ &(\alpha_{2,n}\beta_{1,n+1} + \beta_{1,n}\alpha_{2,n+1} - \alpha_{1,n}\beta_{2,n+1} - \beta_{2,n}\alpha_{1,n+1}) \end{aligned} \right\}, \quad (21)$$

$$A = 2 \sum_{n=0}^{N \rightarrow \infty} (n+1) \left\{ \begin{aligned} &[j_n(x_1)j_{n+1}(x_2) - j_n(x_2)j_{n+1}(x_1)](\beta_{1,n} + \beta_{1,n+1} - \beta_{2,n} - \beta_{2,n+1}) \\ &+ [j_n(x_2)n_{n+1}(x_1) - n_n(x_1)j_{n+1}(x_2)](\alpha_{1,n} + \alpha_{1,n+1}) \\ &+ [j_n(x_1)n_{n+1}(x_2) - n_n(x_2)j_{n+1}(x_1)](\alpha_{2,n} + \alpha_{2,n+1}) \\ &+ [j_n(x_2)n_{n+1}(x_1) - n_n(x_1)j_{n+1}(x_2) + j_n(x_1)n_{n+1}(x_2) - n_n(x_2)j_{n+1}(x_1)] \\ &(\alpha_{1,n}\alpha_{2,n+1} + \alpha_{2,n}\alpha_{1,n+1} + \beta_{1,n}\beta_{2,n+1} + \beta_{2,n}\beta_{1,n+1}) \\ &+ [j_n(x_2)j_{n+1}(x_1) - j_n(x_1)j_{n+1}(x_2) + n_n(x_2)n_{n+1}(x_1) - n_n(x_1)n_{n+1}(x_2)] \\ &(\alpha_{1,n}\beta_{2,n+1} + \beta_{2,n}\alpha_{1,n+1} - \beta_{1,n}\alpha_{2,n+1} - \alpha_{2,n}\beta_{1,n+1}) \end{aligned} \right\}, \quad (22)$$

where $x_1 = k_1 a$ and $x_2 = k_2 a$. The first and second terms in Eq. (18) are the steady components of radiation force caused by each individual plane wave while (Γ) and (A) represent the dynamic component of the radiation force function at the beating frequency $\Delta \omega$.

Finally, from Eq. (16), the dynamic force can be rewritten as

$$\begin{aligned} \langle F_d \rangle &= \pi a^2 \rho k_1 k_2 |A|^2 \sqrt{\Gamma^2 + A^2} \cos(\Delta \omega t - \Phi) \\ &= \pi a^2 \langle E_d \rangle Y_d \cos(\Delta \omega t - \Phi), \end{aligned} \quad (23)$$

where we define the *dynamic energy density* and *dynamic radiation force function* as

$$\langle E_d \rangle = \rho k_1 k_2 |A|^2, \quad (24)$$

$$Y_d = \sqrt{\Gamma^2 + A^2}. \quad (25)$$

The phase shift of the dynamic radiation force with respect to the incident field is given by

$$\Phi = \tan^{-1} \left(\frac{\Gamma}{A} \right). \quad (26)$$

Eq. (23) describes the general formula of the dynamic radiation force. For a known amount of energy $\langle E_d \rangle$, and modulation frequency $\Delta\omega$, and for a known target, (i.e. S_c has a constant value) the only factor that varies and gives a direct evaluation of the oscillatory force is the dynamic radiation force factor Y_d .

2.3. Special cases

2.3.1. The frequencies of the incident waves are equal

When the frequencies of the incoming plane waves are identical, $x_1 = x_2 = x$, $\alpha_{1,n} = \alpha_{2,n}$, $\beta_{1,n} = \beta_{2,n}$ and the incident waves are equivalent to a single plane wave with its amplitude doubled. Consequently, its energy is quadrupled and hence, the radiation force has a four times higher amplitude.

Eq. (16) becomes:

$$\langle F_z \rangle = \pi a^2 \left(\frac{1}{2} \rho k_1^2 |A|^2 \right) Y_{p_1} + \pi a^2 \left(\frac{1}{2} \rho k_2^2 |A|^2 \right) Y_{p_2} + \pi a^2 (\rho k_1 k_2 |A|^2) A, \quad (27)$$

Thus, it can be verified that $\Gamma = 0$ and $A = Y_{p_1} = Y_{p_2} = Y_p$ and Eq. (27) becomes

$$\langle F_x \rangle = 4 \left[\pi a^2 \left(\frac{1}{2} \rho k^2 |A|^2 \right) Y_p \right], \quad (28)$$

and the expression of Y_p is identical to the one given by Hasegawa et al. [12].

2.3.2. Viscoelastic shells

The theory previously established, deals with the dynamic acoustic radiation force on elastic spherical shells. However, for absorbing materials such as rubber and polymers, the theory should take into account the sound-absorption effect that occurs within the shell's core material. Therefore, it is essential to extend the theory to take into account the attenuation of sound. Sound (or ultrasound) absorption in the solid material of the shell can be included by the standard method of introducing complex wave numbers into the theory [35]. This principle can be directly applied to allow for compressional and shear waves' absorption inside the shell's material. The normalized absorption coefficients for the compressional (i.e. $\gamma_{m,1}$) and shear waves (i.e. $\gamma_{m,2}$), respectively, are constant quantities and independent of frequency, as found in many polymeric materials. In the theory described above, and for polymer-type materials, the terms $x_{m,1}$ and $x_{m,2}$ should be replaced by $\tilde{x}_{i,1}$ and $\tilde{x}_{i,2}$ given by

$$\begin{aligned} \tilde{x}_{m,1} &= x_{m,1}(1 - i\gamma_{m,1}), \\ \tilde{x}_{m,2} &= x_{m,2}(1 - i\gamma_{m,2}). \end{aligned} \quad (29)$$

3. Numerical results and discussion

Eq. (18) shows that the total radiation force due to dual-frequency acoustic waves *is not* the mere linear sum of the

two radiation forces due to the incident waves on the shell. There is a coupling term between the two waves resulting in an additional component which is called the dynamic radiation force given in Eq. (23). It is shown from Eq. (23) that the dynamic radiation force has a time-dependent component varying at the difference frequency of the incident waves. Therefore, in addition to the static radiation forces due to the incident waves, the shell experiences an additional dynamic force beating at $\cos(\Delta\omega t - \Phi)$.

The dynamic radiation force function Y_d is evaluated numerically by the use of Eq. (25) for stainless steel (Figs. 2 and 3) and absorbent lucite (Figs. 4 and 5) spherical shells immersed in water. The mechanical properties of these materials for which graphical results are shown, are listed in Table 1 [12,35]. The dynamic radiation force function Y_d is a coefficient determined by the scattering and absorption properties of the shell and its surrounding medium. It is also a function of $x_1 = k_1 a$ and $x_2 = k_2 a$.

2-D plots of the Y_d function are performed and the results covered the range by $0.1 \leq x_1 \leq 10$ for the case without ($\delta x = |x_2 - x_1| = 0$) and with modulation ($\delta x = |x_2 - x_1| = 0.1$). So when x_1 approaches x_2 , the expression of Y_d is reduced to the static radiation force function Y_p where only one single sound plane wave is presented. For the case of the thin shells in Figs. 2,3, and 5, the Y_d curves were plotted versus a small range of $x_1 = k_1 a$ in order to show clearly the differences that exist when the modulation is considered and when it does not. The increment is chosen to be sufficiently small (10^{-4}) to allow capturing the resonance peaks that are very sharp. It is verified that the shape of the Y_d curves does not vary significantly when the increment value is decreased. It is also essential to extend the maximum index N in the series in Eqs. (21) and (22) to greatly exceed the size parameter x_1 and x_2 to ensure proper convergence.

The calculations were evaluated for four shell's thickness values ($b/a = 0; 0.5; 0.9; \text{ and } 0.99$) and compared for particular cases where the hollow region of the spherical shell is filled with the same fluid (i.e. water) or with a different fluid from that of its exterior (i.e. air).

It is found that the dynamic radiation force function curves for stainless steel (Figs. 2 and 3) have a series of prominent peaks for cases of a shell structure, while curves in the case of solid spheres ($b/a = 0$), the curves have series of dips. The material's mechanical properties, the shell thickness as well as the interior and exterior fluid media influence the positions and magnitudes of the peaks and dips that correspond to the resonance vibrational modes.

Results for the case in which the hollow space is filled with air instead of water show that a series of fine peaks do disappear and the curves become relatively flat, especially for thin absorbing lucite shells (Fig. 5; $b/a \geq 0.9$). These results may be applied to benefit acoustic radiometry [40]. Moreover, one notices the high amplitude values in the radiation force function curves for very thin shells filled with air. The explanation for this behavior is that water inside the hollow region facilitates sound (or ultrasound)

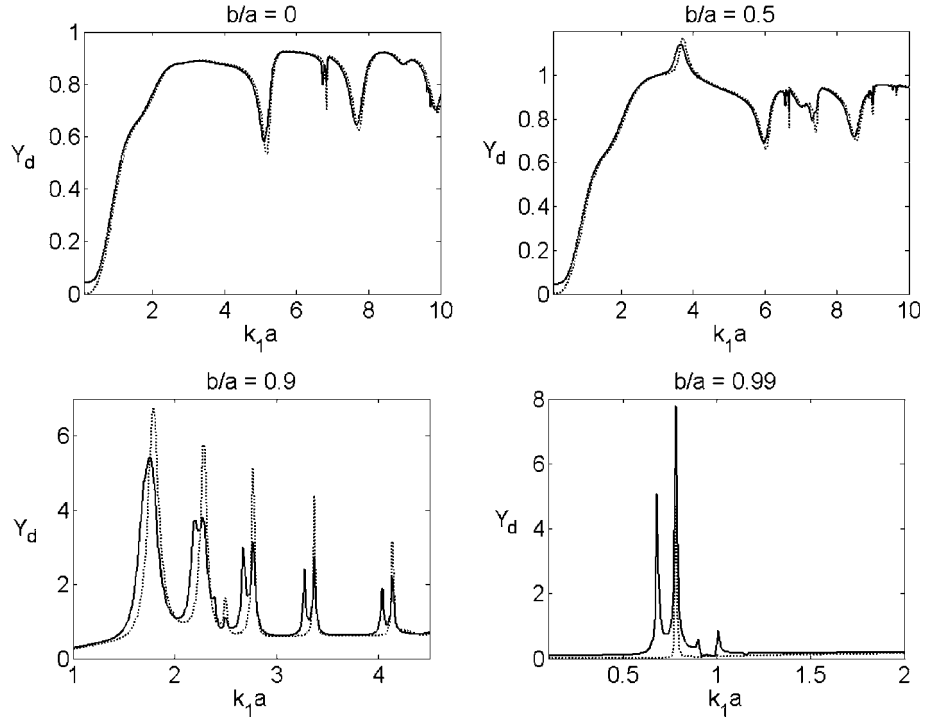


Fig. 2. The dynamic radiation force function curves for spherical stainless steel shells immersed in water. Their interior hollow spaces are also filled with water. The plots are performed for four thickness (b/a) values. The splitting phenomenon is observed at minima and maxima of the curves especially for the thin shells ($b/a \geq 0.9$). Legend: dashed line ($\delta x = 0$, no modulation), and solid line ($\delta x = 0.1$).

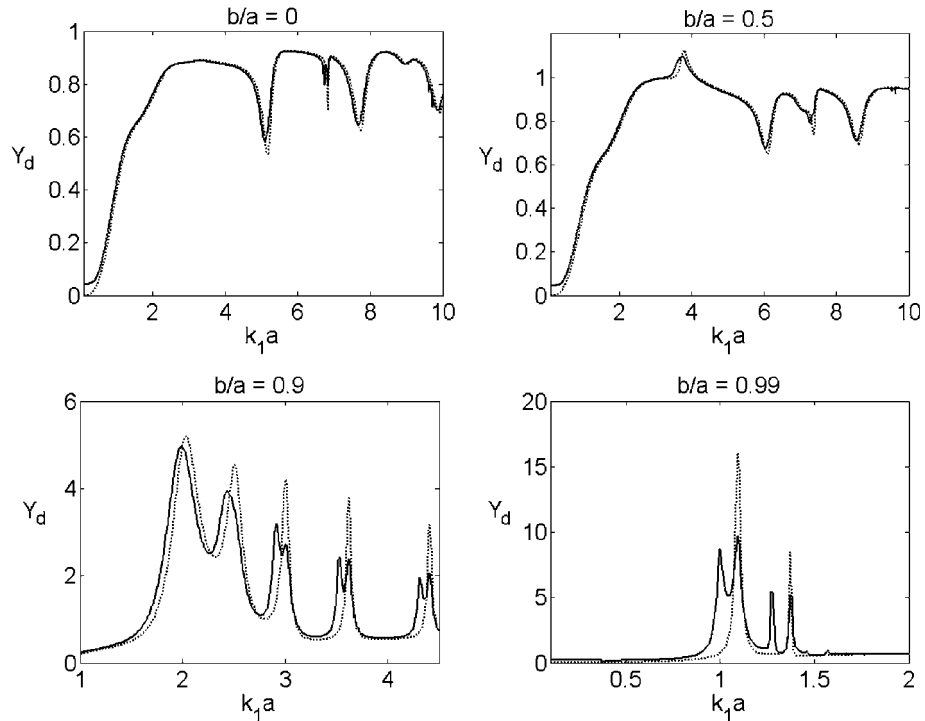


Fig. 3. The same as in Fig. 2 but the shells' interior hollow spaces are filled with air.

transmission through the scattered area, while for the case of air, and since radiation force is proportional to the *gradient* of the energy density that varies significantly due to the large discontinuity of acoustic impedance at the solid-

air interface, the sound reflection is higher. Moreover, for thin shells the surface wave generated along the shell's surface does not penetrate into its volume to create the bulk wave and is reflected. Consequently, the force per

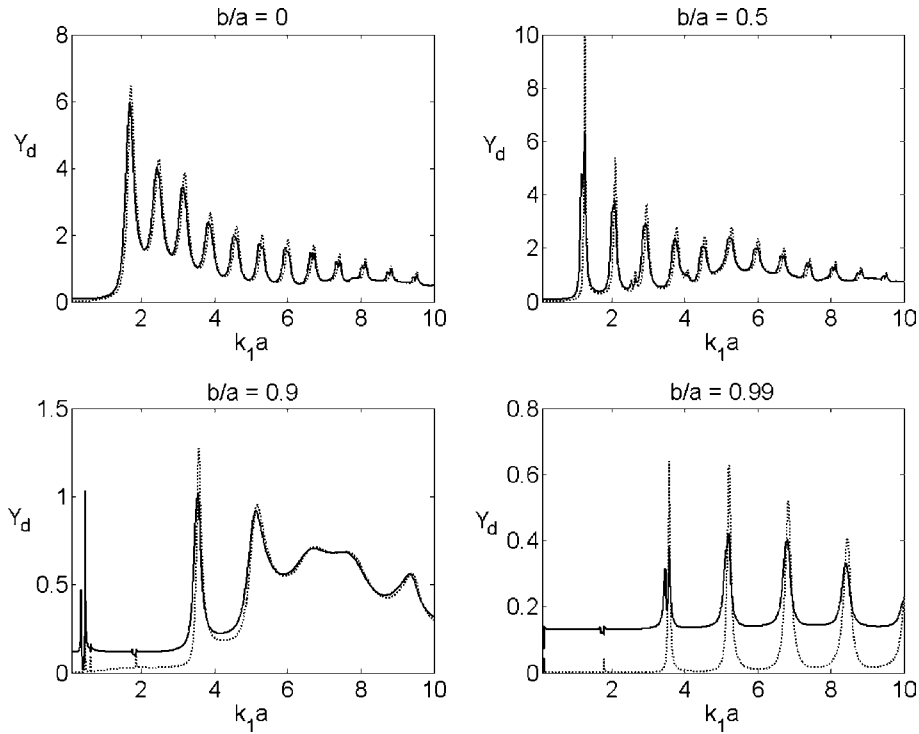


Fig. 4. The dynamic radiation force function curve for *absorbing* lucite spherical shells immersed in water. Their interior hollow spaces are also filled with water. The plots are performed for four thickness (b/a) values. The splitting phenomenon is observed at minima and maxima of the curves especially for the thin shells ($b/a \geq 0.9$). It is particularly noteworthy that resonance peaks are manifested as maxima compared to the case of thick stainless steel shells (Fig. 2). One notices also the change in the radiation force function's amplitude for the thin shells. Legend: dashed line ($\delta x = 0$, no modulation), and solid line ($\delta x = 0.1$).

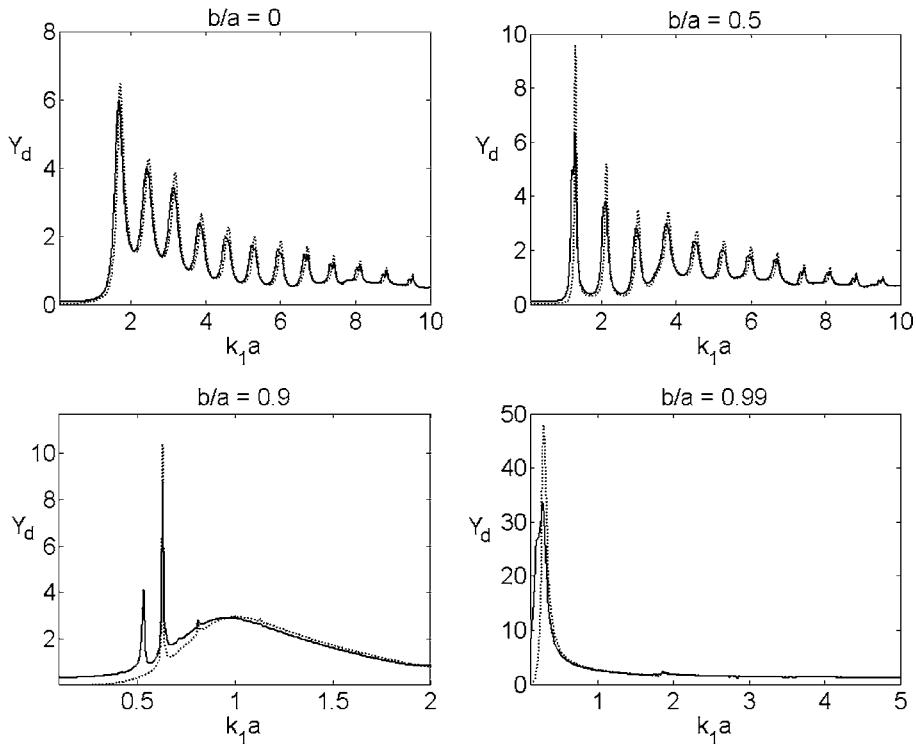


Fig. 5. The same as in Fig. 4 but the shells' interior hollow spaces are filled with air. The results for the thin shells ($b/a \geq 0.9$) show that a series of fine peaks do disappear and the curves become relatively flat as long as the dimensionless size parameter increases (high $k_1 a$). These results may be applied to benefit acoustic radiometry.

Table 1
Mechanical parameters of materials used in the numerical calculations

Material	Mass density [kg/m ³]	Compressional velocity c_1 [m/s]	Shear velocity c_2 [m/s]	$\gamma_{m,1}$	$\gamma_{m,2}$
Lucite	1191	2690	1340	0.0035	0.0053
Stainless steel	7900	5240	2978
Air	1.23	340
Water	1000	1500

cross-sectional area acting on the shell is of high amplitude, which is confirmed by the curves.

An interesting noteworthy fact is the low frequency radiation force enhancement for the lucite shells. The enhancement is not removed by the lucite material absorption. This phenomenon was also observed in acoustic backscattering; the density of lucite is close to that of water (to some extent) and this was seen to have a significant effect on the velocity of Rayleigh waves that produce an acoustic backscattering enhancement from lucite solid spheres [41]. Subsonic Rayleigh waves have lower phase velocities than the bulk waves in the fluid medium surrounding the shell. The most interesting feature of this type of waves is the presence of energy leakage in the subsonic range [42]. Acoustic (back)scattering and radiation force are two different phenomena closely related, since the acoustic scattering coefficients are used to calculate the force (see Eqs. (6) and (25)). These calculations are the first to show this behavior for the case of the dynamic radiation force on absorbent spherical shells.

It is particularly important to note that in the graph of the static radiation force function $Y_{d(\delta x=0)}$ where the curve is relatively flat, a very little change in the $Y_{d(\delta x=0.1)}$ curves is perceived, so that $Y_{d(\delta x=0.1)}$ can be approximated to Y_p (or $Y_{d(\delta x=0)}$) for thick shells ($b/a < 0.9$). However, when δx increases, the value of Y_d starts to deviate from Y_p , which is clearly shown in the figures at the extrema (maxima and minima) of the curves, especially for thin shells ($b/a \geq 0.9$). Calculations not presented here have shown that the splitting of the resonance peaks increases linearly while increasing the modulation size parameter δx . It is particularly noteworthy that the splitting occurs when the modulation size parameter δx starts to exceed the width of the resonance peaks in the Y_p curves. It is also noticeable that the splitting in a resonance peak produces two peaks in the $Y_{d(\delta x=0.1)}$ curves which are separated by a dimensionless frequency shift equal to the modulation dimensionless frequency (i.e. $\delta x = 0.1$). Therefore, the use of the static radiation force function to approximate the dynamic radiation force function is not accurate to any further extent, and it is essential to use the expression of the dynamic radiation force function given by Eq. (25).

4. Conclusion

The major achievement of this work was to calculate theoretically the dynamic radiation force experienced by elastic

and viscoelastic spherical shells placed in an amplitude-modulated sound (or ultrasound) field. Analytical equations that establish relationships between parameters of the medium and the acoustic field were derived. It was shown that the radiation force is no longer static but has a dynamic (oscillatory) component. The results of numerical calculations were presented indicating how the dynamic radiation force function Y_d was affected by variations in the material parameters of the shell. As it was also shown in the figures, the Y_d curves can be approximated by the static radiation force function Y_p in the region where the curves are relatively flat (far from the extrema). However, significant changes in the Y_d curves occurred at their resonance extrema (peaks and dips) when the modulation size parameter δx has started to exceed the width of the resonance peaks in the Y_p curves. Thus, the use of Y_p to approximate Y_d is no longer valid and the expression of the dynamic radiation force should be used. It was also shown that the theory developed here is more broad since it includes the results for solid spheres by simply allowing $b/a = 0$.

References

- [1] R.W.S. Rayleigh, On the pressure of vibration, *Philos. Mag.* 3 (1902) 338–346.
- [2] P.J. Westervelt, The theory of steady forces caused by sound waves, *J. Acoust. Soc. Am.* 23 (1951) 312–315.
- [3] R.T. Beyer, Radiation pressure—the history of a mislabeled tensor, *J. Acoust. Soc. Am.* 63 (1978) 1025–1030.
- [4] A.J. Livett, E.W. Emery, S. Leeman, Acoustic radiation pressure, *J. Sound Vib.* 76 (1981) 1–11.
- [5] R.C. Chivers, L.W. Anson, Calculations of the backscattering and radiation force functions of spherical targets for use in ultrasonic beam assessment, *Ultrasonics* 20 (1982) 25–34.
- [6] W.L. Nyborg, J.A. Rooney, Comments on “Acoustic radiation pressure produced by a beam of sound” [*J. Acoust. Soc. Am.* 72 (1982) 1673–1687], *J. Acoust. Soc. Am.* 75 (1984) 263–264.
- [7] K. Beissner, Two concepts of acoustic radiation pressure, *J. Acoust. Soc. Am.* 79 (1986) 1610–1612.
- [8] C.P. Lee, T.G. Wang, Acoustic radiation pressure, *J. Acoust. Soc. Am.* 94 (1993) 1099–1109.
- [9] L.V. King, On the acoustic radiation pressure on spheres, *Proc. R. Soc. London Ser. A* 147 (1934) 212–240.
- [10] K. Yosioka, Y. Kawasima, Acoustic radiation pressure on a compressible sphere, *Acustica* 5 (1955) 167–173.
- [11] T. Hasegawa, K. Yosioka, Acoustic radiation force on a solid elastic sphere, *J. Acoust. Soc. Am.* 46 (1969) 1139–1143.
- [12] T. Hasegawa, Y. Hino, A. Annou, H. Noda, M. Kato, N. Inoue, Acoustic radiation pressure acting on spherical and cylindrical shells, *J. Acoust. Soc. Am.* 93 (1993) 154–161; See also F.G. Mitri, Theoretical and experimental determination of the acoustic radiation force acting on an elastic cylinder in a plane progressive wave – Far-field derivation approach, *New J. Phys.*, in press.
- [13] F.G. Mitri, Acoustic radiation force acting on absorbing spherical shells, *Wave Motion* 43 (2005) 12–19.
- [14] F.G. Mitri, Frequency dependence of the acoustic radiation force acting on absorbing cylindrical shells, *Ultrasonics* 43 (2005) 271–277.
- [15] F.G. Mitri, Acoustic radiation force acting on elastic and viscoelastic spherical shells placed in a plane standing wave field, *Ultrasonics* 43 (2005) 681–691.
- [16] F.G. Mitri, Theoretical calculation of the acoustic radiation force acting on elastic and viscoelastic cylinders placed in a plane standing or quasistanding wave field, *Eur. Phys. J.B* 44 (2005) 71–78;

- See also W. Wei, D.B. Thiessen, P.L. Marston, Acoustic radiation force on a compressible cylinder in a standing wave, *J. Acoust. Soc. Am.* 116 (2004) 201–208;
 Erratum: *J. Acoust. Soc. Am.* 118 (2005) 551;
 W. Wei, P.L. Marston, Equivalence of expressions for the acoustic radiation force on cylinders (L), *J. Acoust. Soc. Am.* 118 (2005) 3397–3399.
- [17] F.G. Mitri, Acoustic radiation force on cylindrical shells in a plane standing wave, *J. Phys. A: Math. Gen.* 38 (2005) 9395–9404;
 F.G. Mitri, Z.E.A. Fellah, Theoretical calculation of the acoustic radiation force on layered cylinders in a plane standing wave – Comparison of near and far-field solutions, *J. Phys. A: Math. Gen.*, in press.
- [18] F.G. Mitri, Acoustic radiation force due to incident plane-progressive waves on coated spheres immersed in ideal fluids, *Eur. Phys. J. B* 43 (2005) 379–386.
- [19] P.L. Marston, Shape oscillation and static deformation of drops and bubbles driven by modulated radiation stresses—Theory, *J. Acoust. Soc. Am.* 67 (1980) 15–26.
- [20] P.L. Marston, R.E. Apfel, Quadrupole resonance of drops driven by modulated acoustic radiation pressure—experimental properties, *J. Acoust. Soc. Am.* 67 (1980) 27–37.
- [21] J.H. Cantrell Jr., Acoustic-radiation stress in solids. I. Theory, *Phys. Rev. B* 30 (1984) 3214–3220.
- [22] W.T. Yost, J.H. Cantrell Jr., Acoustic-radiation stress in solids. II. Experiment, *Phys. Rev. B* 30 (1984) 3221–3227.
- [23] A.A. Doinikov, Theory of acoustic radiation pressure for actual fluids, *Phys. Rev. E* 54 (1996) 6297.
- [24] M. Greenspan, R.F. Breckenridge, C.E. Tschiegg, Ultrasonic transducer power output by modulated radiation pressure, *J. Acoust. Soc. Am.* 63 (1978) 1031–1038.
- [25] K. Nightingale, M.S. Soo, R. Nightingale, G. Trahey, Acoustic radiation force impulse imaging: in vivo demonstration of clinical feasibility, *Ultras. Med. Biol.* 28 (2002) 227–235.
- [26] A.P. Sarvazyan, O.V. Rudenko, S.D. Swanson, J.B. Fowlkes, S.Y. Emelianov, Shear wave elasticity imaging: a new ultrasonic technology of medical diagnostics, *Ultras. Med. Biol.* 24 (1998) 1419–1435.
- [27] M. Fatemi, J.F. Greenleaf, Ultrasound stimulated vibro-acoustic spectroscopy, *Science* 280 (1998) 82–85.
- [28] M. Fatemi, J.F. Greenleaf, Vibro-acoustography: an imaging modality based on ultrasound-stimulated acoustic emission, *Proc. Natl. Acad. Sci. USA* 96 (1999) 6603–6608.
- [29] F.G. Mitri, P. Trompette, J.Y. Chapelon, Detection of object resonances by vibro-acoustography and numerical vibrational mode identification, *J. Acoust. Soc. Am.* 114 (2003) 2648–2653.
- [30] M. Fatemi, J.F. Greenleaf, Application of radiation force in noncontact measurement of the elastic parameters, *Ultrason. Imaging* 21 (1999) 141–154.
- [31] F.G. Mitri, Inverse determination of porosity from object’s resonances, *J. Appl. Phys.* 96 (2004) 5866–5869.
- [32] S. Chen, M. Fatemi, J.F. Greenleaf, Remote measurement of material properties from radiation force induced vibration of an embedded sphere, *J. Acoust. Soc. Am.* 112 (2002) 884–889.
- [33] F.G. Mitri, J.F. Greenleaf, M. Fatemi, Chirp imaging vibro-acoustography for removing the ultrasound standing wave artifact, *IEEE Trans. Med. Imag.* 24 (2005) 1249–1255.
- [34] F.G. Mitri, P. Trompette, J.Y. Chapelon, Improving the use of vibro-acoustography for brachytherapy metal seed imaging: A feasibility study, *IEEE Trans. Med. Imag.* 23 (2004) 1–6.
- [35] F.G. Mitri, S. Chen, Theory of dynamic acoustic radiation force experienced by solid cylinders, *Phys. Rev. E* 71 (2005) 016306.
- [36] F.G. Mitri, M. Fatemi, Dynamic acoustic radiation force acting on cylindrical shells: theory and simulations, *Ultrasonics* 43 (2005) 435–445.
- [37] G.T. Silva, S. Chen, J.F. Greenleaf, M. Fatemi, Dynamic ultrasound radiation force in fluids, *Phys. Rev. E* 71 (2005) 056617.
- [38] S. Chen, G.T. Silva, R.R. Kinnick, J.F. Greenleaf, M. Fatemi, Measurement of dynamic and static radiation force on a sphere, *Phys. Rev. E* 71 (2005) 056618;
 See also S. Chen, Shear property characterization of viscoelastic media using vibrations induced by ultrasound radiation force, Ph.D. thesis, Mayo Graduate School 2002.
- [39] J.A. Rooney, Does radiation pressure depend on B/A? *J. Acoust. Soc. Am.* 54 (1973) 429–430.
- [40] T. Hasegawa, K. Yosioka, Acoustic radiation force on fused silica spheres, and intensity determination, *J. Acoust. Soc. Am.* 58 (1975) 581–585.
- [41] B.T. Hefner, P.L. Marston, Backscattering enhancements associated with subsonic Rayleigh waves on polymer spheres in water: observation and modeling for acrylic spheres, *J. Acoust. Soc. Am.* 107 (2000) 1930–1936;
 F.G. Mitri, Z.E.A. Fellah, J.Y. Chapelon, Acoustic backscattering form function of absorbing cylinder targets, *J. Acoust. Soc. Am.* 115 (2004) 1411–1413.
- [42] V.G. Mozhaev, M. Weihnacht, Subsonic leaky Rayleigh waves at liquid–solid interfaces, *Ultrasonics* 40 (2002) 927–933.